npg

ORIGINAL ARTICLE

Regulation of AMPA receptor surface trafficking and synaptic plasticity by a cognitive enhancer and antidepressant molecule

H Zhang[1,2], L-A Etherington[3], A-S Hafner[1,2], D Belelli[3], F Coussen[1,2], P Delagrange[4], F Chaouloff[5], M Spedding[4], JJ Lambert[3], D Choquet[1,2] and L Groc[1,2]

The plasticity of excitatory synapses is an essential brain process involved in cognitive functions, and dysfunctions of such adaptations have been linked to psychiatric disorders such as depression. Although the intracellular cascades that are altered in models of depression and stress-related disorders have been under considerable scrutiny, the molecular interplay between antidepressants and glutamatergic signaling remains elusive. Using a combination of electrophysiological and single nanoparticle tracking approaches, we here report that the cognitive enhancer and antidepressant tianeptine (S 1574, [3-chloro-6-methyl-5, 5-dioxo-6,11-dihydro-(c,f)-dibenzo-(1,2-thiazepine)-11-yl) amino]-7 heptanoic acid, sodium salt) favors synaptic plasticity in hippocampal neurons both under basal conditions and after acute stress. Strikingly, tianeptine rapidly reduces the surface diffusion of AMPA receptor (AMPAR) through a Ca^{2+}/calmodulin-dependent protein kinase II (CaMKII)-dependent mechanism that enhances the binding of AMPAR auxiliary subunit stargazin with PSD-95. This prevents corticosterone-induced AMPAR surface dispersal and restores long-term potentiation of acutely stressed mice. Collectively, these data provide the first evidence that a therapeutically used drug targets the surface diffusion of AMPAR through a CaMKII–stargazin–PSD-95 pathway, to promote long-term synaptic plasticity.

INTRODUCTION

The ability of neuronal circuits and associated connections to adapt their activity in response to salient environmental stimuli is a vital process for most organisms. Recently, it has become evident that psychiatric pathologies, such as depression, are accompanied by a compromised neuroplasticity, which refers to the ability of an adult brain to adapt functionally and structurally to internal and external stimuli, in important regions such as the hippocampus, amygdala and prefrontal cortex.[1] Although the monoaminergic neurotransmitters are undoubtedly involved in depression, recent investigations have highlighted the role of an imbalance between fast neurotransmitters, such as glutamate, and neuromodulators.[2] Glutamatergic transmission has an important function in the plasticity of neuronal connections and circuits and is implicated in learning and memory processes in the brain structures such as the hippocampus. In glutamatergic synapses, the ionotropic AMPA receptor (AMPAR) mediates the majority of fast transmission and changes in its trafficking have been proposed to be a core mechanism for synaptic plasticity. Functional imaging and histological studies revealed deficits in glutamatergic signaling in patients with depression.[3] Treatment with antidepressants, such as the selective serotonin reuptake inhibitor fluoxetine, or the mononamine reuptake inhibitor imipramine, increases the phosphorylation of AMPAR, a molecular process observed during synaptic plasticity, suggesting that these glutamate receptors are linked to the therapeutic impact of the antidepressants.[4,5] Thus, although the action of most antidepressants

is to increase the availability of biogenic amines (for example, serotonin, noradrenaline), it is likely that their therapeutic benefits result from an interplay between monoaminergic and glutamatergic signaling that leads to neuronal adaptations and increased excitatory synapse plasticity.[6–8]

Serving as the basis of several animal models of depression,[9–11] the molecular, cellular and behavioral effects of acute and chronic stress in the brain are complex. Indeed, severe stressors reduce neuroplasticity such as synaptic long-term plasticity and the dendritic structure in brain areas involved in important cognitive functions (for example, hippocampus and prefrontal cortex).[12–15] A single exposure to an elevated platform (that is, acute stress) can cause a long-lasting alteration of synaptic plasticity.[10,16] Among the cellular consequences of such a stress is the phosphorylation status of proteins involved in glutamatergic signaling, such as AMPAR, NMDAR and Ca^{2+}/calmodulin-dependent protein kinase II (CaMKII). Consistently, acute stress or response to stress hormones (for example, noradrenaline, corticosterone) alters the trafficking of AMPAR, modifying the plastic range of glutamate synapses[16–18] and memory encoding processes.[16,17] In basal conditions, AMPAR are trafficked to/from the plasma membrane of neurons in extrasynaptic/perisynaptic area from which they laterally diffuse to the postsynaptic area.[19–23] It recently emerged that corticosterone exposure increases GluA1- and GluA2-AMPAR synaptic content through an increase in lateral diffusion.[24,25] Thus, corticosterone appears to modulate the plastic range of glutamatergic synapses through changes in AMPAR surface trafficking,

[1]Interdisciplinary Institute for Neuroscience, University of Bordeaux, UMR 5297, Bordeaux, France; [2]CNRS, IINS UMR 5297, Bordeaux, France; [3]Division of Neuroscience, Medical Research Institute, Ninewells Hospital and Medical School, University of Dundee, Dundee, UK; [4]Institut de Recherches Servier (IdRS), Experimental Sciences, Suresnes, France and [5]NeuroCentre INSERM U862, Université de Bordeaux, Bordeaux, France. Correspondence: Dr L Groc or Dr D Choquet, Interdisciplinary Institute for Neuroscience, Universite de Bordeaux, UMR 5297, 33000 Bordeaux, France.
E-mail: laurent.groc@u-bordeaux2.fr or daniel.choquet@u-bordeaux2.fr

which thus emerges as a potential primary target for antidepressants and future depression-related therapeutic strategies.

Tianeptine (S 1574, [3-chloro-6-methyl-5,5-dioxo-6,11-dihydro-(c,f)-dibenzo-(1,2-thiazepine)-11-yl) amino]-7 heptanoic acid, sodium salt) is a drug known to act as a memory enhancer as its administration increases long-term memory in rodents.[26–28] In addition, tianeptine acts as an antidepressant with structural similarities to the tricyclic antidepressant agents, but with different pharmacological properties.[29,30] Indeed, the monoaminergic hypothesis of antidepressant action cannot account for all the properties of this drug, which is presently classified as a glutamatergic antidepressant. Tianeptine does not bind to adrenergic, dopaminergic or serotoninergic receptors or transporters,[31] but, through still unknown mechanisms, it reverses synaptic plasticity, dendritic atrophy, memory impairment and neuronal loss in stress conditions.[9,32–35] Thus, tianeptine triggers cellular cascades that favor neuronal adaptations and plasticity, which likely sustain antidepressant efficacy. Tianeptine alters glutamatergic transmission, increasing for instance the phosphorylation of GluA1 subunits,[36] and counteracts stress-induced changes in excitatory synaptic transmission in the hippocampus through altered protein phosphorylation in the postsynaptic compartment.[37] In addition, tianeptine potentiates AMPA receptors by activating CaMKII and protein kinase A via the p38, p42/44 MAPK and JNK pathways.[38] Because AMPAR surface dynamics recently emerged as an important cellular process for glutamate synapse plasticity under basal and stress conditions, here we used tianeptine to dissect out the surface glutamatergic pathway activated by this memory enhancer and antidepressant. We uncovered that tianeptine is a potent modulator of AMPAR surface diffusion, preventing the altered surface trafficking changes induced by the stress hormone corticosterone and restoring plasticity in hippocampal synapses previously compromised by acute stress or corticosterone. At the molecular level, tianeptine modulates the surface diffusion of AMPAR through a CaMKII-dependent mechanism that favors the binding of the AMPAR auxiliary subunit stargazin to PDZ scaffold proteins.

MATERIALS AND METHODS

Primary neuronal cultures, transfection and drugs
Cultures of hippocampal neurons were prepared from E18 Sprague–Dawley rats following a previously described method.[39–41] Briefly, cells were plated at a density of $100–200 \times 10^3$ cells per 60 mm dish on poly-lysine pre-coated coverslips. Cultures were maintained in serum-free neurobasal medium (Invitrogen, Paris, France) and kept at 37 °C in 5% CO_2 for 20 days *in vitro* (DIV) at maximum. Cells were transfected with appropriate plasmids using Effectene (Qiagen, Paris, France). For live cell imaging, cells were transfected at DIV 7 and 8 and imaged at DIV 15–17; for a single nanoparticle (quantum dot (QD)), tracking cells were transfected at DIV 9 and 10 and imaged at DIV 11 and 12; for Förster resonance energy transfer (FRET)/fluorescence lifetime imaging microscopy (FLIM) imaging, cells were transfected at DIV 7 and 8 and imaged at DIV 9 and 10. Tianeptine was a gift from Servier (Suresne, France); KN93 was from Calbiochem (Paris, France).

Plasmid construct
Homer1c::GFP and homer1c::DsRed were generated by subcloning homer1c cDNA into the eukaryotic expression vector pcDNA3 (Invitrogen); either eGFP or DsRed was inserted at the N terminus of the homer1c sequence. GluA1::SEP was generated by subcloning GluA1 cDNA into eukaryotic expression vector prK5; SEP was inserted at the N terminus of the GluA1 sequence. Wild-type (WT) stargazin::GFP and mutant stargazin ΔC::GFP were generated by inserting eGFP into WT stargazin and stargazin ΔC constructs. Stargazin ΔC was generated by deleting the final four amino acids of stargazin constructs corresponding to the PDZ binding site. Inducible WT stargazin and stargazin S9A (StA) were generated by subcloning WT stargazin and StA cDNA (nine serines at the putative

CaMKII/PKC phosphorylation sites were mutated to alanines) into the eukaryotic expression vector pBI tet-on GFP. Doxycycline (2 μg ml^{-1}) was used to induce protein expression during a 16–24 h period. Stargazin::tetracysteine (Stg::4cys) was generated by inserting tetracysteine tag into WT stargazin at position 302 (−21 position) (mouse, UniProtKB/Swiss-Prot O88602) using directed mutagenesis (QuickChange II XL Site-Directed Mutagenesis Kit; Stratagene, Amsterdam, The Netherlands). WT stargazin cDNA was in the eukaryotic expression vector pcDNA. Tetracysteine_5F, 5′-GTCAGTACCGGTTTTCTGAACTGCTGCCCAGGTTGCTGCATGGAGCCAGCTAGCGTCAGT-3′ and tetracysteine_6R, 5′-ACTGACGCTAGCTGGCTCCATGCAGCAACCTGGGCAGCAGTTCAGAAAACCGGTACTGAC-3′ were used as sense and antisense primers. WT PSD-95::eGFP was generated by subcloning PSD-95 cDNA into the eukaryotic expression vector pcDNA; eGFP was inserted at position 253 on PSD-95.

Live cell and fluorescence recovery after photobleaching imagin
Live cell imaging was used to visualize the intensity of surface GluA1-AMPARs; hippocampal neurons were co-transfected with GluA1::SEP and homer1c::DsRed and imaged at DIV 15–17. Then, a spinning-disk microscope Leica DMI6000 (Leica Microsystems, Wetzlar, Germany) equipped with a confocal Scanner Unit CSU22 (Yokogawa Electric Corporation, Tokyo, Japan) and with an HCX PL Apo ×63 oil NA 1.4 objective and a Quantem camera (Photometrics, Tucson, AZ, USA) was used to image surface GluA1-AMPARs. The diode lasers used were at 473 and 532 nm. The z stacks were done with a piezo P721.LLQ (Physik Instrumente (PI), Karlsruhe, Germany). The motorized stage used is a Scan IM (Märzhäuser, Wetzlar, Germany). The 37 °C atmosphere was created with an incubator box and an air heating system (Life Imaging Services, Basel, Switzerland). Acquisitions were carried out on the MetaMorph software (Molecular Devices, Sunnyvale, CA, USA). Fluorescence recovery after photobleaching (FRAP) of GluA1::SEP was used to measure ensemble AMPAR mobility. Hippocampal neurons were co-transfected with GluA1::SEP and homer1c::DsRed and imaged at DIV 15–17. The FRAP experiments were carried out with a 100 mW Saphire laser at 488 nm (Coherent Laser Group, Santa Clara, CA, USA) or a 50 mW 405 nm laser scanner FRAP system (Roper Scientific, Evry, France) and a Quantem camera (Photometrics). The objective used was an HCX PL Apo ×63 oil NA 1.4. Diffraction-limited regions expressing GluA1::SEP were photobleached for 5 ms. Recovery from photobleach was monitored by 150 s consecutive acquisitions at 0.5 Hz and normalized to the fluorescence measured before the photobleach. The images were corrected for background noise and continuous photobleaching using the MetaMorph software. Recovery curves were normalized to the fluorescence measured before the bleach and residual fluorescence right after the bleach was set to zero.

Single nanoparticle (QD) tracking and surface diffusion calculation
For endogenous GluA2 QD tracking, hippocampal neurons were either incubated with monoclonal antibody against N-terminal extracellular domain GluA2 subunit (MAB397; Millipore, Paris, France) for 10 min, followed by 5 min incubation with QD 655 goat F(ab')2 anti-mouse IgG (Invitrogen), or neurons were incubated for 10 min with the premix of QD 655 goat anti-mouse IgG and monoclonal antibody Fab fragment against N-terminal extracellular domain of GluA2 subunit (kind gift from K Keinänen, University of Helsinki, Helsinki, Finland). Nonspecific binding was blocked by additional casein (Vector Laboratories, Eagleville, PA, USA) to the QD 15 min before use. QDs were detected by using a mercury lamp and appropriate excitation/emission filters. Images were obtained with an interval of 50 ms and up to 1000 consecutive frames. Signals were detected using a CCD camera (Quantem; Roper Scientific). QDs were followed on randomly selected dendritic regions for up to 20 min. QD recording sessions were processed with the Metamorph software (Universal Imaging Corp, Sunnyvale, CA, USA). The instantaneous diffusion coefficient, D, was calculated for each trajectory, from linear fits of the first 4 points of the mean square displacement vs time function using $MSD(t) = <r^2>(t) = 4Dt$. The two-dimensional trajectories of single molecules in the plane of focus were constructed by correlation analysis between consecutive images using a Vogel algorithm. QD-based

trajectories were considered synaptic if colocalized with homer1c dendritic clusters for at least five frames.

Fluorescence internalization assays

Translocation of AMPARs from cell surface to intracellular compartments was visualized and quantified by an 'antibody feeding' immunofluorescence internalization assay in hippocampal neurons cultured at DIV 15–17 as described with minor modification. Neurons were labeled for 8 min at 37 °C with an antibody directed against the extracellular region of GluA2 subunit (kind gift from E Gouaux, HHMI, NY, USA). After brief washing, neurons were incubated at 37 °C in conditioned growth medium containing vehicle or pharmacological agents. Neurons were fixed for 5 min at room temperature in 4% paraformaldehyde/4% sucrose without permeabilization, and stained with fluorescein isothiocyanate-conjugated secondary antibodies for 1 h at room temperature, to visualize pre-labeled surface receptors. Neurons were then permeabilized for 5 min 0.1% Triton X-100 at room temperature and stained with Cy3-conjugated secondary antibodies for 1 h at room temperature, to visualize pre-labeled internalized receptors. Red fluorescence intensities indicative of internalization were divided by total (red + green) fluorescence intensities. Units of internalization were measured as red/total fluorescence normalized to controls.

ReAsH labeling

ReAsH is commercially available from Invitrogen as TC-ReAsH. Hippocampal culture neurons expressing PSD-95::eGFP (donor) and HA::stargazin (HA::Stg) or Stg::4cys constructs for 30 h were incubated with ReAsH 2.5 μM (acceptor) in OPTI-MEM (Gibco, Paris, France) for 30 min at 37 °C with 5% CO_2. To reduce signal-to-noise ratio, cells were then washed twice in OPTI-MEM containing 100 × BAL wash buffer for 5 min.

FLIM experiments

FLIM experiments were performed at 37 °C using an incubator box with an air heater system (Life Imaging Services) installed on an inverted Leica DMI6000B (Leica Microsystem) spinning disk microscope and using the LIFA frequency domain lifetime attachment (Lambert Instruments, Roden, The Netherlands) and the LI-FLIM software. Cells were imaged with an HCX PL Apo × 100 oil NA 1.4 objective using an appropriate GFP filter set. Cells were excited using a sinusoidally modulated 1-W 477 nm LED (light-emitting diode) at 40 MHz under wild-field illumination. Emission was collected using an intensified CCD LI2CAM camera (FAICM; Lambert Instruments). The phase and modulation were determined from a set of 12 phase settings using the manufacturer's LI-FLIM software. Lifetimes were referenced to a 1 mM solution of fluorescein in saline (pH 10) that was set at 4.00 ns lifetime. Lifetime values are a mean of 12 synaptic regions and 6 dendritic regions per neuron. Following FLIM measurements, cells were excited using a 100 mW 491 nm DPSS laser (Calypso; Cobolt, Stockholm, Sweden) for GFP imaging and a 100 mW 561 nm DPSS lasers (Jive; Cobolt) for ReAsH imaging, and imaged with an HCX PL Apo CS × 63 oil NA 1.4 objective. Signals were recorded with a back-illuminated Evolve EMCCD camera (Photometrics). Acquisitions were carried out on the software MetaMorph (Molecular Devices).

Mouse hippocampal slice preparation

Hippocampal slices were obtained from 2- to 4-month-old male C57/BL6 mice. Such mice were killed by cervical dislocation. Note all procedures involving mice were performed in accordance with Schedule 1 of the UK Government Animals (Scientific Procedures) Act 1986 and under the auspices of the approved Home Office project license. Following decapitation, the brain was rapidly dissected, with incisions made at the cerebellum and frontal lobes, and then placed in an incubation chamber containing artificial cerebrospinal fluid (aCSF) of the following composition (in mM): NaCl, 124; KCl, 3; $CaCl_2$, 2; $NaHCO_3$, 26; NaH_2PO_4, 1.25; D-glucose, 10; $MgSO_4$, 1; pH 7.4 with 95% O_2/5% CO_2. The temporal aspects of the brain were trimmed, bisected and then glued to a metal plate, such that the mid-line was uppermost and horizontal. In this orientation, the brain was submerged in oxygenated (95% O_2/5% CO_2) aCSF and a Vibratome

(IntraCel, Royston, Herts, UK) was used to cut 400-μm-thick brain slices. Saggital hippocampal brain slices were cut from each bisected hemisphere, which were then placed on a submerged nylon mesh in an incubation chamber, filled with circulating oxygenated aCSF, at room temperature, for at least 1 h before use.

Ex vivo extracellular recording from hippocampal CA1 pyramidal neurons

A hippocampal slice was transferred to a submersion recording chamber (Scientific Systems Design, Paris, France) and continuously perfused at 4–6 ml min^{-1} with aCSF utilizing a peristaltic pump (Gilson Minipuls Evolution, Paris, France). The perfusion medium was gassed with 95% O_2/5% CO_2 and maintained at 31 °C. For the accurate positioning by micromanipulators of the stimulating and recording electrodes, the hippocampal slice was viewed via a microscope (Olympus SZ30). To induce and monitor basal synaptic transmission, a Teflon-coated tungsten bipolar stimulating electrode (~100 μm in diameter) was positioned in stratum radiatum, allowing the afferent Schaffer collateral–commissural pathway from the CA3 area to the CA1 region to be stimulated. A Digitimer stimulator was utilized to excite this pathway at 30 s intervals (that is, 0.033 Hz, 100 μS duration). The glass (King Precision Glass; ID: 1.00 ± 0.05; OD: 1.55 ± 0.05) extracellular recording microelectrode was filled with aCSF (< 5 MΩ) and positioned in the stratum radiatum of area CA1. This microelectrode was carefully lowered into the dendritic region of CA1 until clear field excitatory postsynaptic potentials (fEPSPs) were observed. Such fEPSPs were simultaneously displayed on an oscilloscope (Tektronix 2201 digital storage oscilloscope) and via an A to D converter (National Instruments, Paris, France; BNC-2090) on a computer screen. The slope of each fEPSP (mV ms^{-1}) was calculated online and the stimulus adjusted to produce a response 40% of the maximum. For LTP experiments, maximal or submaximal LTP was induced by a theta-burst stimulation (TBS) protocol (4 or 3 pulses, respectively, delivered at 100 Hz, repeated 10 times, at an interval of 200 ms). The stimulus parameters, the acquisition and the analysis of fEPSPs were under the control of LTP software (courtesy of Dr Anderson and Professor Collingridge, Bristol University, UK; http://www.ltp-program.com). The electrical signals were acquired at 10 kHz and filtered at 10 Hz–3 kHz. Statistical analysis of LTP was performed using the SPSS statistical software and comparisons of the magnitude of LTP were measured by means of repeated measures linear regression analysis at 50–60 min after the TBS.

Drugs and application protocol

Tianeptine and KN93 were prepared as a stock solution of 10 mM in milli-Q water and dimethylsulfoxide, respectively, and subsequently diluted into the perfusion saline to the desired final bath concentration. For all studies, stable baseline recordings of fEPSPs (0.033 Hz monitored as the slope of the fEPSP on line) were obtained for a minimum of 10 min before experimentation. To determine the impact of tianeptine, or KN93, on basal excitatory neurotransmission, the drug was perfused onto the brain slice for 20 min and the slope of the fEPSP monitored throughout the experimental period. To assess whether KN93 influenced the effect of tianeptine on the basal fEPSP, the tissue was pre-incubated with KN93 for 20 min, before co-application with tianeptine for a further 20 min. To investigate whether tianeptine influenced LTP, it was again applied for 20 min (allowing for any effects of the drug on basal excitatory neurotransmission to reach equilibrium), before delivering the TBS. The drug was then continually perfused throughout the remainder of the LTP experiment (a further 60 min). For the experiments on corticosterone, the steroid was pre-incubated with the tissue for 20 min. Subsequently, fEPSPs (pre–post the TBS protocol) were recorded in the continued presence of corticosterone. The influence of tianeptine on the effect of corticosterone on LTP was assessed by co-incubating tianeptine with corticosterone for a further 20 min before delivery of the 4-pulse TBS.

Acute stress protocol

The behavioral stress protocol was adapted from Rocher et al.[10] Briefly, acute stress exposure involved placing the mice on an open elevated

platform for 45 min, immediately following this challenge the mice were killed by cervical dislocation and hippocampal brain slices were prepared as described above.

Statistics

For imaging data, statistical values are given as mean ± s.e.m. or medians ± interquartile range) defined as the interval between 25 to 75% percentile. Statistical significances were tested using Prism 4.0 (GraphPad, San Diego, CA, USA). Normally distributed data sets were compared using the paired Student's t-test and unpaired Student's t-test. Statistical significance between more than two normally distributed data sets was tested by one-way analysis of variance test, followed by a Newman–Keuls test to compare individual pairs of data. Non-Gaussian data sets were tested by non-parametric Mann–Whitney test. Indications of significance correspond to P-values < 0.05 (*), $P < 0.01$ (**) and $P < 0.001$ (***).

RESULTS

Tianeptine decreases GluA1- and GluA2-AMPAR surface diffusion but not endocytosis

AMPARs are heteromeric proteins composed of different combinations of subunits drawn from a repertoire of GluA1, GluA2, GluA3 or GluA4 subunits.[42] The trafficking of AMPAR in neurons has been thoroughly investigated over the past two decades, primarily because the regulation of the AMPAR synaptic content has emerged as an important mechanism for glutamatergic synaptic plasticity.[23] It is now accepted that AMPARs are trafficked to/from the synapses through lateral diffusion in the plasma membrane and exocytosis/endocytosis.[40,43–47] To investigate the effect of the antidepressant tianeptine on AMPAR signaling, we first tested whether the drug modified the surface diffusion of GluA2-AMPAR (the vast majority of surface AMPAR) in hippocampal neurons. To this aim, we used the single nanoparticle tracking approach in which a QD is coupled to an antibody specific for the extracellular domain of the endogenous GluA2 subunit[48] (Figure 1a). Surface GluA2-AMPARs were tracked in both extrasynaptic and synaptic compartments of DIV 11 and 12 cultured hippocampal neurons. In the basal condition, endogenous GluA2-AMPARs were rather diffusive, exploring large areas of the dendritic tree[40,43–47] (Figure 1b, left panel). Incubation with tianeptine (10 or 100 μM, 10–30 min) significantly decreased the surface diffusion of extrasynaptic GluA2-AMPAR (Figures 1b and c). In the synapse, GluA2-AMPAR surface diffusion was further decreased by tianeptine (Figures 1b and d). These changes in surface diffusion were partially due to an increased fraction of immobile GluA2-AMPAR (surface diffusion $< 0.005 \, \mu m^2 \, s^{-1}$): from 20% after vehicle to 31% after 100 μM tianeptine (Figure 1d, right panel; the first point of the distribution corresponds to the fraction of immobile receptors). It should be noted that a shorter incubation time with tianeptine (5 min incubation + 10 min withdrawal) was sufficient to significantly reduce GluA2-AMPAR surface diffusion (Supplementary Figure 1). As reported previously,[41] an increased endocytosis of AMPAR is accompanied by a marked decrease in receptor surface diffusion. To test whether tianeptine also acted on the AMPAR internalization rate, we measured the GluA2 subunit internalization rate in the presence of tianeptine (10 or 100 μM). In basal conditions, GluA2-AMPAR constitutively internalized at a rate of approximately 40%/30 min (Supplementary Figure 2), confirming previous observations.[40] The presence of 10 and 100 μM tianeptine did not affect the internalization rate of GluA2-AMPAR. Collectively, these data indicate that tianeptine greatly decreased the surface diffusion of AMPAR, particularly in synapses, thereby stabilizing the receptors within the postsynaptic area.

Because the single particle approach only informs on the behavior of a single receptor and because AMPAR composed of different subunits can be differentially trafficked,[23] we investigated whether tianeptine affected the surface trafficking of the GluA1-AMPAR population. To do so, we used FRAP in hippocampal neurons co-transfected with GluA1::SEP and homer1c::DsRed (postsynaptic density marker of glutamatergic synapses) (Figure 2a). SEP is a pH-sensitive variant of enhanced GFP that exhibits bright fluorescence when exposed to neutral pH (for example, extracellular environment), but that has relatively little fluorescence when exposed to low pH (for example, internal acidified vesicles).[49] Thus, the fluorescence observed in neurons transfected with GluA1::SEP mainly originates from surface GluA1-AMPAR. Compared to vehicle, tianeptine (10 and 100 μM) decreased the amount of GluA1-SEP fluorescence recovery in the extrasynaptic and synaptic compartments (Figure 2b). We quantified the mobile fraction of each group, which is considered as the relative fluorescence recovery at the end of FRAP (elapse time 150 s). In accordance with the above GluA2-QD data, tianeptine at 10 and 100 μM decreased the ensemble mobility of GluA1-AMPAR. Moreover, the reduction in surface diffusion was higher in the synaptic area (Figures 2b and c). Taken together, these data demonstrate that tianeptine, at physiologically relevant concentrations,[30] greatly reduced the surface diffusion of AMPAR at both single molecule and ensemble levels.

Tianeptine's effects on AMPAR surface diffusion require CaMKII activity

CaMKII is critically required for the synaptic recruitment of AMPAR during plasticity as well as development.[46] Among the various intracellular cascades activated by tianeptine, phosphorylation of the GluA1 subunit is essential.[36,50] In addition, tianeptine activates CaMKII and protein kinase A via the p38, p42/44 MAPK and JNK pathways.[38] Because CaMKII is a potent regulator of AMPAR subunit phosphorylation,[51] and because acute stress models alter the phosphorylation status of CaMKII,[52] here we investigated whether tianeptine's effects on AMPAR surface diffusion required CaMKII activity. The CaMKII inhibitor, KN93 (10 μM), was co-applied with tianeptine (10 or 100 μM), and the consequences of these treatments on GluA2-AMPAR surface diffusion were assessed using both single particle tracking (Figure 3a) and FRAP of the GluA1-SEP subunit (Figures 3b and c). Remarkably, the presence of KN93 (10 μM) fully rescued the decrease in GluA2-AMPAR surface diffusion induced by tianeptine at 10 μM (Figure 3a, left panel) and at 100 μM (Figure 3a, right panel) in the synaptic compartments. We observed a similar trend for the extrasynaptic compartment (data not shown). This result was further confirmed using the FRAP approach on neurons transfected with GluA1::SEP. Indeed, the effects of tianeptine (10 or 100 μM) on GluA1-AMPAR fluorescence recovery were prevented by the presence of KN93 (Figures 3b and c). In line with the results shown in Figure 3a, KN93 also fully rescued the decreased ensemble mobility of AMPAR observed after tianeptine (Figures 3b and c). Taken together, these data demonstrate that tianeptine acts on GluA-AMPAR surface trafficking through a CaMKII-dependent pathway.

Phosphorylation of stargazin and its binding to PSD-95 mediates tianeptine's effects on AMPAR surface diffusion

The CaMKII-induced AMPAR immobilization requires both phosphorylation of the AMPAR auxiliary subunit stargazin and its binding to scaffold proteins of the postsynaptic density, such as PSD-95.[46] In addition, previous studies have shown that synaptic recruitment of AMPAR can be triggered by phosphorylation of the stargazin C terminus domain.[53,54] To further explore the molecular cascade downstream of CaMKII activation in tianeptine's regulation of AMPAR surface diffusion, we expressed various stargazin mutants in neurons and tested their impact on tianeptine's effects. First, we expressed the dephosphorylated stargazin S9A mutant (StA), for which nine serines at the putative CaMKII/PKC phosphorylation sites are mutated to alanines. The expression of StA but not WT stargazin prevented the tianeptine-induced decrease in
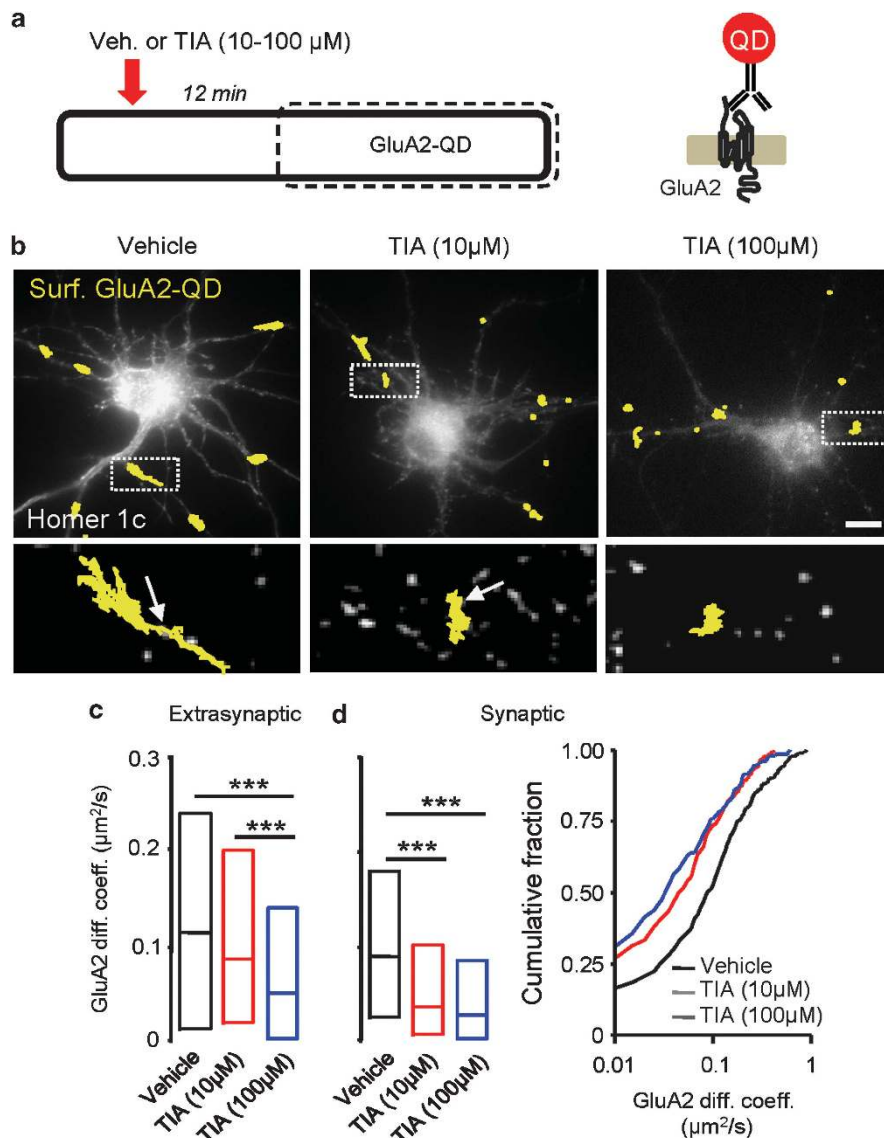
Figure 1. GluA2-AMPAR surface diffusion is rapidly decreased by tianeptine (TIA) application. (**a**) Experimental scheme showing that 12 min after the incubation of TIA, surface GluA2-AMPARs were tracked for 20 min in the extrasynaptic and synaptic compartments of days *in vitro* (DIV) 11–12 cultured hippocampal neurons using quantum dot (QD) coupled to the antibody specific for the extracellular domain of endogenous GluA2 subunit. (**b**) Typical QD trajectory (yellow) in neurons treated with vehicle (left panel), TIA (10 μM) (middle panel) and TIA (100 μM) (right panel). (Lower panels) Enlarged single GluA2-AMPAR-QD trajectories. The arrows represent homer1c cluster, that is, synapses. Scale bar = 10 μm. (**c**) Diffusion coefficients (median ± 25–75% interquartile range (IQR)) of extrasynaptic GluA2-AMPARs was decreased in neurons incubated with TIA (10 and 100 μM) compared to vehicle-treated neurons (vehicle = 0.11 ± 0.022–$0.24\,\mu m^2\,s^{-1}$, $n = 753$; TIA (10 μM) = 0.087 ± 0.025–$0.20\,\mu m^2\,s^{-1}$, $n = 446$; TIA (100 μM) = 0.055 ± 0.007–$0.142\,\mu m^2\,s^{-1}$, $n = 255$; ***$P < 0.001$). (**d**) Synaptic GluA2-AMPAR diffusion coefficient was also decreased after TIA incubation (10 and 100 μM) (vehicle = 0.08 ± 0.03–$0.18\,\mu m^2\,s^{-1}$, $n = 281$; TIA (10 μM) = 0.04 ± 0.01–$0.11\,\mu m^2\,s^{-1}$, $n = 245$; TIA (100 μM) = 0.03 ± 0.007–$0.09\,\mu m^2\,s^{-1}$, $n = 214$; ***$P < 0.001$). (Right panel) Cumulative distributions of diffusion coefficients of neurons treated with vehicle or TIA (10 and 100 μM). Note the shift toward the left in the presence of TIA, indicating a reduced GluA2-AMPAR surface diffusion immobilized at synapses.

AMPAR surface diffusion (Figure 4a). This finding indicates that the phosphorylation of stargazin is essential for tianeptine-induced AMPAR stabilization. Because the phosphorylation of stargazin enhances the interaction between stargazin and PSD-95, which in turn immobilizes AMPAR,[43] we next examined the role of the interaction between stargazin and PSD-95 in mediating tianeptine's effects. To this aim, hippocampal neurons were transfected with either WT stargazin or a mutant stargazin (ΔC Stg) in which the last four C terminus amino acids corresponding to the PDZ binding site of PSD-95 were deleted.[43] In ΔC Stg- but not in WT stargazin-expressing neurons, tianeptine failed to reduce

GluA2-AMPAR surface diffusion (Figure 4b), suggesting that the interaction between stargazin and PSD-95 is essential for the tianeptine-induced stabilization of surface AMPAR.

Tianeptine increases the interaction between stargazin and PSD-95 through CaMKII activation

To ensure the tianeptine's effects on AMPAR lateral mobility are a result of stargazin interaction with PSD-95, we monitored this interaction by FRET– FLIM in living hippocampal culture neurons (9 DIV). For this, neurons were transfected with PSD-95∷GFP and
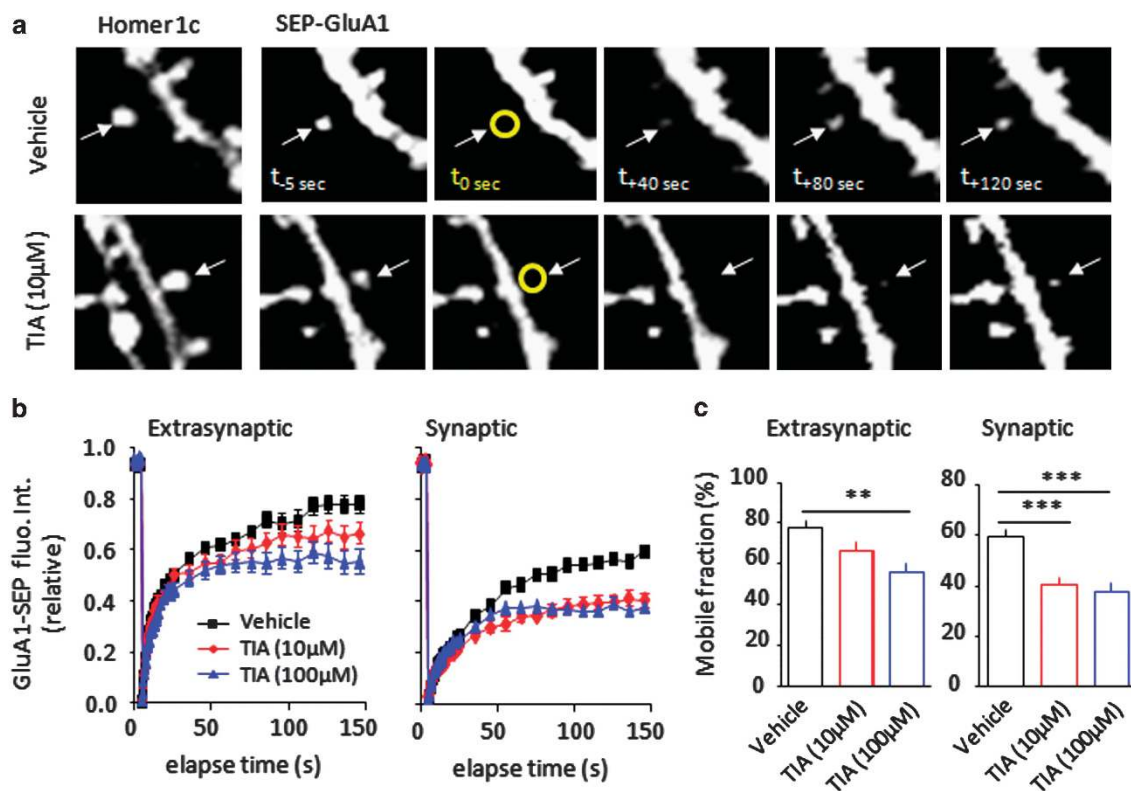
Figure 2. Tianeptine (TIA) reduces the surface diffusion of GluA1-AMPAR. (**a**) Typical time-lapse images during fluorescence recovery after photobleaching (FRAP) in hippocampal neurons co-transfected with homer1c::DsRed and GluA1::SEP. Homer1c::DsRed image (very left panel) was recorded 5 s before photobleaching. The rest were GluA1::SEP images 5 s before photobleaching (t_{-5s}), at photobleaching (t_{0s}) and 40, 80, 120 s after photobleaching (t_{+40s}, t_{+80s}, t_{+120s}). White arrows indicate a typical synaptic area. (**b**) Quantified relative fluorescence intensity recovery during 150 s at extrasynaptic (left panel) and synaptic (right panel) compartments. Compared to vehicle, TIA (10 and 100 μM) slowed down GluA1-SEP fluorescence recovery in the extrasynaptic and synaptic compartments. (**c**) Quantified GluA1-AMPARs mobile fraction at extrasynaptic (left panel) and synaptic (right panel) compartments. The mobile fraction was considered as the percentage of fluorescence recovery at the end of FRAP (elapse time 150 s) (vehicle = 78 ± 3.5%, n = 24; TIA (10 μM) = 66 ± 4.4%, n = 21; TIA (100 μM): 55 ± 4.9%, n = 21; right panel, vehicle = 60 ± 2.5%, n = 44; TIA (10 μM) = 40 ± 2.8%, n = 30; TIA (100 μM) = 38 ± 1.9%, n = 20; **P < 0.01; ***P < 0.001).

stargazinStg::4cys (Figure 5a). GFP is used as a donor fluorophore able to transfer its energy to ReAsH, a red fluorophore that binds specifically to tetracysteine tags[55] (Figure 5a). A reduction in GFP lifetime indicates that GFP efficiently transfers its energy to ReAsH and that two proteins directly interact. The degree of FRET is estimated as a function of GFP lifetime decrease. After ReAsH incubation, PSD-95::GFP lifetime was significantly decreased in neurons co-expressing PSD-95::GFP and Stg::4cys compared to neurons co-expressing PSD-95::GFP and HA::Stg while it is similar between cells expressing PSD::GFP alone or with HA::Stg (Figure 5c), suggesting that ReAsH specifically FRET when bound to Stg::4cys and so that PSD-95::GFP interacts directly with Stg::4cys. We then examined effects of tianeptine on Stg::4cys's binding to PSD-95::GFP in synaptic (Figure 5d) and extrasynaptic (Figure 5e) compartments. Notably, PSD-95::GFP lifetime in the absence of drug was much lower in synapses (Figure 5d) compared to extrasynaptic compartments (Figure 5e), indicating that Stg::4cys in basal condition binds PSD-95::eGFP in extra-synaptic areas, but the interaction is mainly synaptic. Tianeptine dramatically decreased PSD-95::GFP lifetime in both synaptic and extrasynaptic compartments, indicating that tianeptine increased the interaction between Stg::4cys and PSD-95::GFP (Figures 5d and e). Consistent with single and ensemble tracking experiments (Figure 3), KN93 (10 μM) rescued tianeptine's effect on PSD-95::GFP lifetime, partially in synapses (69% of the initial lifetime was rescued) (Figure 5d) and fully in extrasynaptic

compartments (Figure 5e), implying that the interaction of PSD-95 and stargazin was downstream of CaMKII. Interestingly, KN93 alone had no effect extrasynaptically (Figures 5d and e) but reduced stargazin-PSD-95 interaction in synapses (Figures 5e and d), which was consistent with a previous report that KN93 alone increased GluA2-AMPAR lateral mobility in synapses.[46] All together, our FRET-FLIM data prove that tianeptine increases the interaction between PSD-95 and stargazin both synaptically and extrasynaptically in a CaMKII-dependent manner.

Tianeptine enhances field EPSPs and AMPAR synaptic content in hippocampal neurons

The above data strongly suggest that tianeptine can impact on AMPAR synaptic signaling through changes in AMPAR surface trafficking. Indeed, tianeptine has previously been reported to increase the amplitude of AMPA-mediated signaling in CA3 hippocampal neurons.[37,38] To dissect the mechanisms involved in such processes, the effect of 3–50 μM tianeptine on submaximal fEPSPs (elicited at 0.033 Hz) recorded from mouse hippocampal CA1 neurons was first determined. Tianeptine (10 and 50 μM) increase the fEPSP slope (40 ± 9% increase, n = 4 and 69 ± 13% increase, n = 3), when measured at equilibrium (~8 and 20 min, respectively, after bath perfusion) (Figures 6a and b). It was noted that a lower concentration of tianeptine (3 μM) was ineffective (1.2 ± 1% increase, n = 6) in this respect. Interestingly, 10 μM KN93

fully prevented the tianeptine (10 μM)-induced increase in the fEPSP (4 ± 4% increase, n = 5; Figure 6b), indicating that the activation of CaMKII is a necessary step in this process.

To test whether changes in glutamate receptor synaptic content could explain the tianeptine-induced increase in fEPSP, we measured the content of GluA1 subunit content in the extrasynaptic and synaptic membrane compartments of living neurons. Cultured hippocampal neurons were co-transfected with GluA1::SEP (Super Ecliptic pHluorin at extracellular N termini) and homer1c::DsRed and imaged at DIV 15–17 (Figure 6c). A 30-min incubation with vehicle did not significantly affect the content of surface GluA1-AMPAR at synapses (colocalization with homer1c) or at extrasynaptic compartments (Figures 6c and d). In contrast, incubation of neurons with tianeptine (10 μM, 30 min) significantly increased the GluA1-AMPAR intensity in synapses (Figures 6c and d). The extrasynaptic content was not significantly altered, although a tendency towards an increased content was noted

($P = 0.06$; Figure 6d). Increasing the concentration of tianeptine (100 μM) upregulated the surface content of GluA1-AMPAR both in the synaptic (0 min: 50 ± 2.5 arbitrary unit (a.u.), n = 6; 30 min: 62 ± 5 a.u., n = 6; $P < 0.05$) and in the extrasynaptic (0 min: 105 ± 8 a.u., n = 6; 30 min: 132 ± 14 a.u., n = 6; $P < 0.05$) compartments. Taken together, these data indicate that tianeptine increased the synaptic, with little or no effect on the extrasynaptic content of GluA1-AMPAR, supporting a model in which tianeptine dynamically modulates glutamate transmission in the hippocampus through changes in AMPAR content.

Acute stress or corticosterone suppresses hippocampal CA1 LTP in vitro, a deficit reversed by tianeptine

Because AMPAR surface trafficking is highly involved in glutamate synaptic adaptations,[24,44,45,47] the possibility that tianeptine not only modulates the basal surface trafficking of AMPAR and consequently synaptic excitatory transmission, but also alters the plastic range of glutamate synapses in stress is of interest. In support, tianeptine has been reported to enhance hippocampal LTP in vivo.[15,50] To explore the in vitro effect of tianeptine on long-term plasticity and to identify whether tianeptine increases the magnitude of LTP, or the stimulus threshold at which LTP is induced, we measured fEPSPs in acute hippocampal slices (Figure 7a). Delivery of a 4-pulse TBS protocol to the CA1 region of hippocampal slices induced a robust form of LTP determined 50 min post-TBS (Figure 7b). A 3-pulse TBS protocol was significantly less effective in this respect (Figures 7a and b). The influence of tianeptine (10 μM) on submaximal LTP induced by a 3-pulse TBS was determined after the effect of this drug on the control fEPSP (Figures 7a and b) had reached equilibrium (that is, 20 min drug incubation before tetanus). This concentration of tianeptine greatly increased submaximal LTP, but had no significant effect ($P > 0.05$) on LTP induced by the 4-pulse TBS (Figure 7b). Note, 3 μM tianeptine, a concentration that had no effect on the slope of control fEPSPs, similarly greatly enhanced submaximal (3-pulse TBS) LTP (control = 20 ± 6%, n = 6; tianeptine = 87 ± 19%, n = 6; $P < 0.05$). Collectively, these data indicate that tianeptine facilitates LTP in hippocampal CA1 circuits, probably by reducing the threshold for its induction.
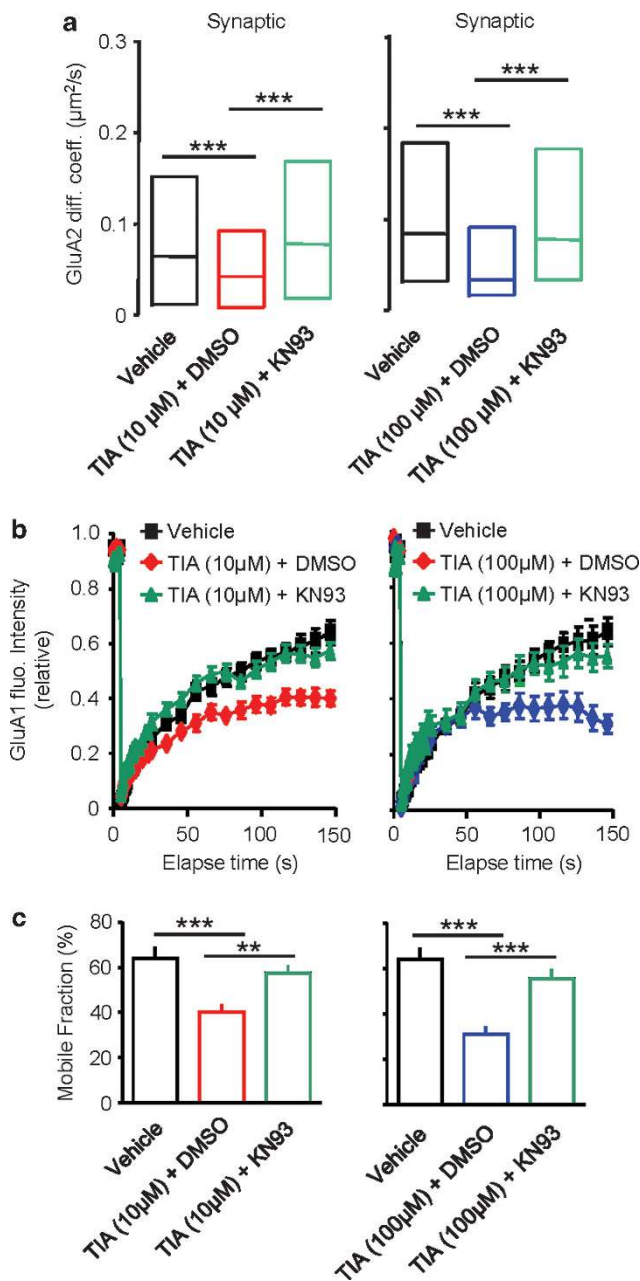
Figure 3. Tianeptine (TIA)-induced GluA-AMPA receptor (AMPAR) surface diffusion decrease is a Ca^{2+}/calmodulin-dependent protein kinase II (CaMKII)-dependent mechanism. (**a**) Surface GluA2-AMPARs were tracked in the synaptic compartments of days in vitro (DIV) 11–12 cultured hippocampal neurons in the presence/absence of TIA (10 μM) (left panel) and of 100 μM TIA (right panel) with or without CaMKII inhibitor, KN93 (10 μM) (median ± 25–75% interquartile range (IQR); vehicle = 0.06 ± 0.01–0.15 $\mu m^2 s^{-1}$, n = 276; TIA (10 μM) + DMSO = 0.04 ± 0.01–0.1 $\mu m^2 s^{-1}$, n = 210; TIA (10 μM) + KN93 = 0.08 ± 0.02–0.17 $\mu m^2 s^{-1}$, n = 244; ***$P < 0.001$; right panel: vehicle = 0.09 ± 0.03–0.19 $\mu m^2 s^{-1}$, n = 198; TIA (100 μM) + DMSO = 0.04 ± 0.01–0.13 $\mu m^2 s^{-1}$, n = 155; TIA (100 μM) + KN93 = 0.08 ± 0.03–0.19 $\mu m^2 s^{-1}$, n = 173; ***$P < 0.001$). (**b**) Ensemble AMPAR mobility was assessed by fluorescence after photobleaching (FRAP) at synaptic compartments in the presence/absence of TIA (10 μM) (left panel) and of TIA (100 μM) (right panel) with or without CaMKII inhibitor, KN93 (10 μM). The decreased GluA1-AMPAR fluorescence recovery induced by TIA (10 or 100 μM) was fully restored in the presence of KN93. (**c**) Quantified GluA1-AMPARs mobile fraction at synaptic compartments in vehicle, TIA and TIA + KN93 conditions. The mobile fraction was considered as the percentage of fluorescence recovery at the end of FRAP (elapse time 150 s) (left panel: vehicle = 64 ± 4.7%, n = 26; TIA (10 μM) = 40 ± 3.2%, n = 21; TIA (10 μM) + KN93 = 57 ± 3%, n = 32; right panel: vehicle = 64 ± 4.7%, n = 26; TIA (100 μM) = 31 ± 3.6%, n = 24; TIA (100 μM) + KN93 = 55 ± 4.4%, n = 18; **$P < 0.01$; ***$P < 0.001$). DMSO, dimethylsulfoxide.
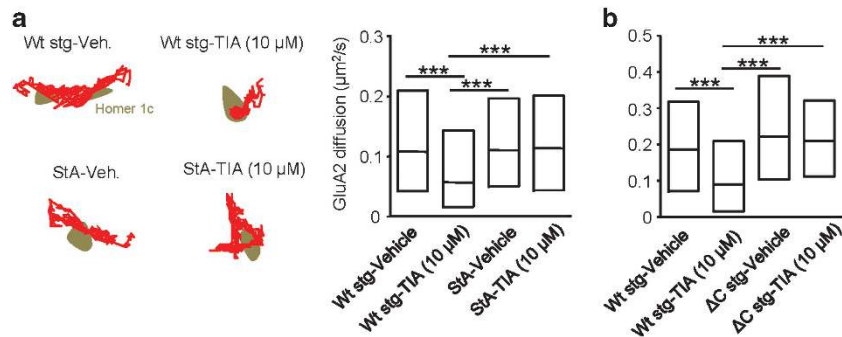
Figure 4. The phosphorylation of stargazin and its PDZ binding site are required to mediate tianeptine's (TIA's) effects on AMPA receptor (AMPAR) surface diffusion. (**a**) Global (extrasynaptic and synaptic) surface GluA2-AMPAR were tracked in days *in vitro* (DIV) 11–12 cultured hippocampal neurons transfected with wild-type stargazin (WT Stg) and dephosphorylated stargazin S9A mutant (StA) from which nine serines at the putative Ca^{2+}/calmodulin-dependent protein kinase II/protein kinase C (CaMKII/PKC) phosphorylation sites were mutated to alanines. In WT Stg-expressing cells, TIA (10 µM) significantly decreased the GluA2-AMPAR lateral diffusion, while in StA-expressing cells this effect was fully blocked (right panel) (median ± 25–75% interquartile range (IQR); WT Stg-vehicle = $0.10 ± 0.04–0.21\,µm^2\,s^{-1}$, n = 454; WT Stg-TIA (10 µM) = $0.05 ± 0.01–0.15\,µm^2\,s^{-1}$, n = 365; StA-vehicle = $0.11 ± 0.05–0.20\,µm^2\,s^{-1}$, n = 424; StA-TIA (10 µM) median = $0.11 ± 0.04–0.20\,µm^2\,s^{-1}$, n = 563; ***P < 0.001). The left panel shows typical quantum dot (QD) trajectories in the four groups. (**b**) Global surface GluA2-AMPAR were tracked in DIV 11–12 cultured hippocampal neurons transfected with WT Stg or a mutant stargazin (ΔC Stg) in which the last four C terminus amino acids corresponding to the PDZ binding site of PSD-95 were deleted. In ΔC Stg- but not WT Stg-expressing neurons, TIA failed to reduce GluA2-AMPAR surface diffusion (median ± 25–75% IQR; WT Stg-vehicle = $0.186 ± 0.08–0.32\,µm^2\,s^{-1}$, n = 189; WT Stg-TIA (10 µM) = $0.09 ± 0.02–0.21\,µm^2\,s^{-1}$, n = 241; ΔC Stg-vehicle = $0.22 ± 0.10–0.39\,µm^2\,s^{-1}$, n = 173; ΔC Stg-TIA (10 µM) = $0.20 ± 0.11–0.32\,µm^2\,s^{-1}$, n = 132; ***P < 0.001).

The clinical benefits of tianeptine in depression and anxiety disorders have been paralleled to the positive effects of the drug on the neuroadaptive properties of neurons in animal stress models.[29,30] For instance, tianeptine can elicit *in vivo* an LTP that was previously suppressed by an episode of acute stress.[10] Thus, because tianeptine is a known modulator of stress-related dysfunctions,[15,30,56,57] we tested whether tianeptine can modulate *in vitro* the synaptic plasticity of a mouse subjected previously to acute stress. Acute stress was induced by exposing the mouse to an elevated platform for 45 min before being killed.[10] This protocol produced a significant reduction in the *in vitro* LTP induced by the 4-pulse TBS protocol (control = 94 ± 10% increase, n = 9; 'stressed' = 36 ± 7% increase, n = 12; P < 0.05) (Figures 7c and d). Note that these recordings were made 2–5 h after the termination of the stressful challenge and the subsequent preparation of the hippocampal brain slices, suggesting the perturbation of synaptic plasticity induced by this paradigm is robust and well-maintained *in vitro*. Before investigating the effect of tianeptine on this compromised LTP, we determined its influence on the slope of the fEPSP. In common with control recordings, 3 µM tianeptine had no effect on the fEPSP (2.7 ± 2.0% increase, n = 6), whereas again 10 µM produced an increase of the fEPSP (31 ± 9.4%, n = 8), that was not significantly different from control recordings (Figure 6). Although tianeptine (10 µM) had no significant effect on the LTP induced by the 4-pulse TBS in control mice (Figure 7b), now both 3 and 10 µM tianeptine (3 µM = 74 ± 17% increase, n = 6; 10 µM = 74 ± 13% increase, n = 6) significantly (P < 0.05) enhanced LTP if 'stressed' mice were used (Figure 7), suggesting that tianeptine positively modulates the plastic range of glutamate synapses under basal conditions and in the acute stress model. Finally, we tested the direct role of the corticosterone, which is released during stress events, on the same plasticity paradigms. Incubation of the hippocampal slices with corticosterone (10 µM) produced a significant reduction in LTP induced by the 4-pulse TBS protocol (control = 94 ± 10% increase, n = 9; corticosterone = 51 ± 14% increase, n = 4; P < 0.05; Figure 7d), to an extent similar to that observed in stressed mice. Furthermore, 3 µM tianeptine significantly enhanced LTP in the presence of corticosterone (91 ± 6% increase, n = 4, P < 0.05; Figure 7d), strengthening the view that tianeptine positively

modulates the plastic range of glutamate synapses in acute stress conditions.

Tianeptine prevents corticosterone-induced GluA2-AMPAR surface diffusion changes

Previous studies have shown that the stress hormone corticosterone increases the surface trafficking of AMPAR a few hours after exposure,[24,25] a cellular process thought to be crucial for the corticosterone-induced increase in glutamatergic synaptic transmission.[24] We tested the hypothesis that tianeptine restored basal AMPAR trafficking in neurons exposed to corticosterone. To this aim, neurons were incubated with corticosterone or vehicle (phosphate-buffered saline) for 20 min,[24] washed, incubated with tianeptine (10 µM) for 90 min and then imaged using surface GluA2-QD tracking (Figure 8a). Consistent with previous reports of hippocampal neurons,[24,25] corticosterone increased the surface diffusion of GluA2-AMPAR (Figures 8b and c). As exemplified in the trajectories (Figure 8b), GluA2-AMPAR-QDs were more diffusive after corticosterone exposure, exploring larger areas of the dendritic fragment. Strikingly, the application of tianeptine, after corticosterone exposure, fully blocked the corticosterone-induced GluA2-AMPAR surface diffusion increase, both in the extrasynaptic and synaptic compartments (Figure 8c). These data thus indicate that tianeptine stabilizes surface AMPAR in neurons previously exposed to the stress hormone corticosterone. This regulatory mechanism likely prevents the corticosterone-induced accumulation of AMPAR in synapses, which requires a surface translocation of AMPAR from extrasynaptic to synaptic compartments.[24] Thus, tianeptine restores the adaptive potential of glutamate synapses by modulating AMPAR surface diffusion.

DISCUSSION

The molecular and cellular pathways by which antidepressants favor neuroplasticity have been under considerable scrutiny over the past decades.[16] Using a combination of electrophysiological and single nanoparticle tracking approaches here, we report that the antidepressant tianeptine favors synaptic plasticity in CA1 hippocampal neurons both under basal conditions and after an
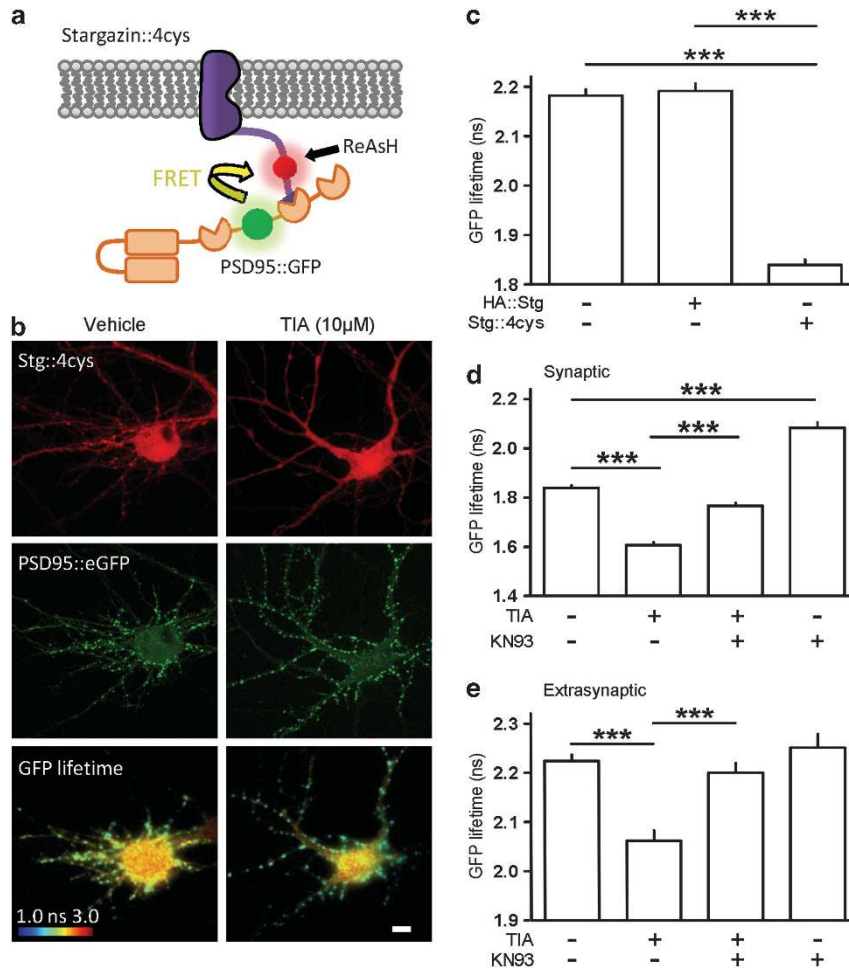
Figure 5. Tianeptine (TIA) enhances stargazin to PSD-95 binding in a Ca^{2+}/calmodulin-dependent protein kinase II (CaMKII)-dependent process. The interaction between stargazin and PSD-95 was studied by Förster resonance energy transfer (FRET)- fluorescence lifetime imaging microscopy (FLIM) in synaptic and extrasynaptic compartments in days in vitro (DIV) 9 cultured hippocampal neurons with or without TIA treatments. (**a**) Experimental schemes showing that neurons were transfected with PSD-95::GFP and stargazin::tetracysteine (Stg::4cys). The site that ReAsH binds to 4cys tags is on the C terminus domain of stargazin 17 amino acids away from the PDZ binding domain. The interaction between stargazin and PSD-95 was monitored by FRET/FLIM, indicated by a decrease in GFP lifetime. (**b**) Sample images of neurons expressing Stg::4cys and PSD-95::GFP with vehicle (left panels) or with TIA treatment (right panels). ReAsH labeling was diffused (top panels). PSD-95::GFP was present in soma, dendrites and clustered in synapses (middle panels). Short lifetime was indicated by blue areas where PSD-95::GFP binds to ReAsH-labeled Stg::4cys (bottom panels). Scale bar = 10 μm. (**c**) Synaptic measurements of PSD-95::GFP lifetime in the presence of ReAsH. GFP lifetime was significantly decreased only in neurons co-expressing Stg::4cys and PSD-95, but not in neurons expressing PSD-95 alone or with HA::stargazin (HA::Stg) (PSD-95::GFP = 2.182 ± 0.013 ns, $n = 14$; PSD-95::GFP/HA::Stg = 2.191 ± 0.015 ns, $n = 14$; PSD-95::GFP/Stg::4cys = 1.839 ± 0.011 ns, $n = 24$; ***$P < 0.0001$). (**d**) Synaptic analysis of PSD-95::GFP lifetime after ReAsH labeling in PSD-95::GFP/Stg::4cys expressing neurons with vehicle or TIA treatment. TIA (10 μM) significantly decreased PSD-95::GFP lifetime (vehicle = 1.839 ± 0.011 ns, $n = 25$; +TIA = 1.607 ± 0.012 ns, $n = 18$; ***$P < 0.0001$). Its synaptic effect was partially blocked by KN93 (10 μM) (TIA + KN93 = 1.767 ± 0.013 ns, $n = 20$; ***$P < 0.0001$). And 10 μM of KN93 alone increased PSD-95::GFP lifetime (KN93 = 2.084 ± 0.021 ns, $n = 4$; ***$P < 0.0001$). (**e**) Extrasynaptic analysis of PSD-95::GFP lifetime after ReAsH labeling in PSD-95::GFP/Stg::4cys expressing neurons with vehicle or TIA treatment. TIA (10 μM) significantly decreased PSD-95::GFP lifetime (vehicle = 2.224 ± 0.013 ns, $n = 25$; +TIA = 2.062 ± 0.021 ns, $n = 18$; ***$P < 0.0001$). Its extrasynaptic effect was fully block by KN93 (10 μM) (TIA + KN93 = 2.200 ± 0.020 ns, $n = 20$; ***$P < 0.0001$). And 10 μM of KN93 had no effect on PSD-95::GFP lifetime (KN93 = 2.251 ± 0.027 ns, $n = 4$; ***$P < 0.0001$). GFP, green fluorescent protein.

acute stress. By measuring the trafficking of single AMPAR, we found that tianeptine greatly stabilizes surface AMPAR. This effect was achieved by reducing their surface diffusion through a CaMKII-dependent mechanism that favors the binding of the AMPAR auxiliary subunit stargazin with PSD-95. This effect prevented corticosterone-induced AMPAR surface dispersal and restored LTP in the hippocampus of acutely stressed mice (Figure 8d). Hence, these data provide the first evidence that the antidepressant tianeptine strongly reduces the surface diffusion of AMPAR through a CaMKII-stargazin-PSD-95 pathway,

which favors long-term synaptic plasticity in basal conditions as well as after either acute stress or after acute incubation with the stress hormone corticosterone.

AMPAR are composed of a combination of GluA1, GluA2, GluA3 and/or GluA4 subunits, which provide different activation and signaling properties.[58] Most AMPARs in hippocampal neurons are heterodimers composed of either GluA1/GluA2 or GluA2/GluA3 subunit combinations.[58] Activity-induced changes in glutamatergic signaling represent the core cellular substrate for experience-driven neuronal adaptations during learning and memory
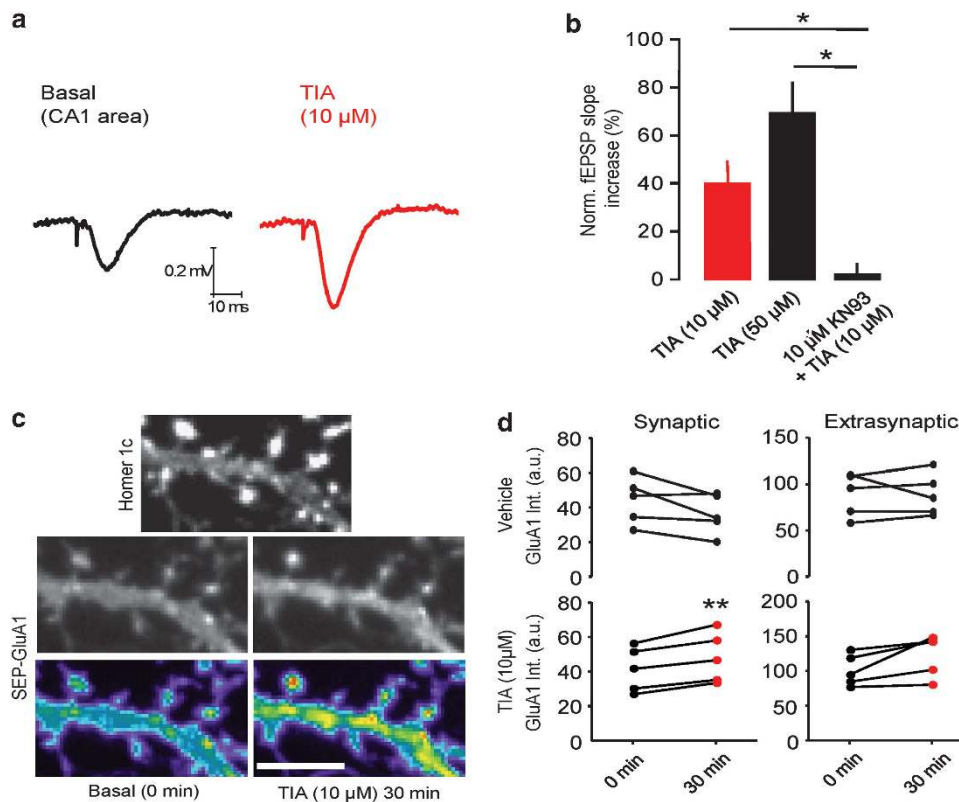
Figure 6. Tianeptine increases excitatory transmission and AMPA receptor (AMPAR) synaptic content. (**a**) Control field excitatory postsynaptic potentials (fEPSPs) were generated by stimulation (0.033 Hz) of the afferent Schaffer collateral–commissural pathway from the CA3 area to the CA1 region. Illustrated is a representative trace of an fEPSP before (black) and after (red) tianeptine (10 μM; 30 min). (**b**) A histogram demonstrating the increase of the slope of the fEPSP (% of the control fEPSP) produced by 10 and by 50 μM tianeptine. Note that the increase of the fEPSP produced by tianeptine (10 μM) is completely prevented by pre-treatment with the Ca^{2+}/calmodulin-dependent protein kinase II (CaMKII) inhibitor KN93 (10 μM). Each bar represents the mean ± s.e.m. of 3–4 independent experiments. (**c**) Sample live fluorescence images of neurites coexpressing homer1c::DsRed (top panels) as postsynaptic density marker of glutamatergic synapses and GluA1::SEP (middle panels) indicating surface AMPARs before (left panels) and 30 min after (right panels) tianeptine application. The bottom panels were GluA1::SEP images in pseudocolor. Scale bar, 10 μm. (**d**) Quantified GluA1::SEP intensity at synaptic (colocalization with the postsynaptic protein, homer1c) and extrasynaptic compartments from paired experiments. Each point represents the mean of GluA1::SEP intensity from 10 to 12 regions before ('0 min'; left points) or 30 min after (right points) tianeptine/vehicle application. The 30-min incubation with vehicle (H_2O) (top panels) did not significantly affect GluA1::SEP intensity at synapses (0 min: 44 ± 5.9 arbitrary unit (a.u.), $n = 5$; 30 min = 36 ± 5 a.u., $n = 5$) or in the extrasynaptic compartment (0 min: 89 ± 10.3 a.u., $n = 5$; 30 min ± 89 ± 10 a.u., $n = 5$). Incubation of neurons with tianeptine (10 μM, 30 min) (bottom panels) significantly increased GluA1::SEP intensity at synapses (0 min: 41 ± 5.7 .u., $n = 5$; 30 min = 48 ± 6.5 a.u., $n = 5$; **$P < 0.01$). The extrasynaptic content was not significantly altered, but a tendency toward an increase content was clearly noted (0 min = 101 ± 10 a.u., $n = 5$; 30 min = 123 ± 13 a.u., $n = 5$; $P = 0.06$). a.u., arbitrary unit.

processes.[59] During plasticity, changes in the content of AMPAR have been well documented.[20,23,60] The AMPAR constitutively cycle in and out of the postsynaptic membrane at rapid, albeit different, rates and changes to this cycling would mediate activity-dependent perturbations of glutamate signaling during plasticity.[20] The content of surface AMPAR mostly depends on endocytosis/exocytosis processes, which internalize or insert, respectively, AMPAR to extra-perisynaptic sites.[20] Once in the plasma membrane, AMPAR diffuse freely, explore large areas of dendrites and exchange between extrasynaptic and synaptic locations with a rather rapid turnover.[40,41,47,61,62] Functionally, the surface diffusion of synaptic AMPAR tunes the plastic range of synapses.[17,62] Recent work shows that the majority of AMPARs incorporated into synapses during LTP is from surface diffusion while exocytosed receptors likely serve to replenish the extra-synaptic pool available for subsequent bouts of plasticity.[45] Among the physiological adaptations for which this process is required, we recently uncovered that corticosteroids (for example, corticosterone in rodents) affect synaptic plasticity through changes in surface AMPAR diffusion.[16,17] The application of corticosterone

on CA1 pyramidal cells increased glutamatergic synaptic transmission (that is, the amplitude of miniature excitatory postsynaptic currents) and prevented the induction of LTP.[63,64] In fact, corticosterone exposure gradually increased the plasma membrane delivery of AMPAR, mostly at extrasynaptic sites, and the consequent fast surface diffusion facilitates the synaptic accumulation of these receptors, occluding LTP. Our current data indicate that after corticosterone exposure, the increase in AMPAR surface trafficking can be pharmacologically modulated by tianeptine in a CaMKII- and PSD-95/stargazin-dependent mechanism. Although tianeptine (10 μM) itself slightly increases the synaptic content of GluA1 (Figure 6d), an effect that may underlie the increase in the basal fEPSP, it does not affect the magnitude of maximal LTP (induced by 4-pulse TBS), but does enhance submaximal LTP (induced by 3-pulse TBS) (Figure 7), implying that tianeptine may enhance the recruitment of AMPAR to synapses during LTP. Because the synaptic delivery of AMPAR involved an intracellular trafficking, an insertion/internalization to the plasma membrane, and a lateral diffusion at the neuronal surface,[23] it is likely that tianeptine acts on the last step of the AMPAR cellular journey to
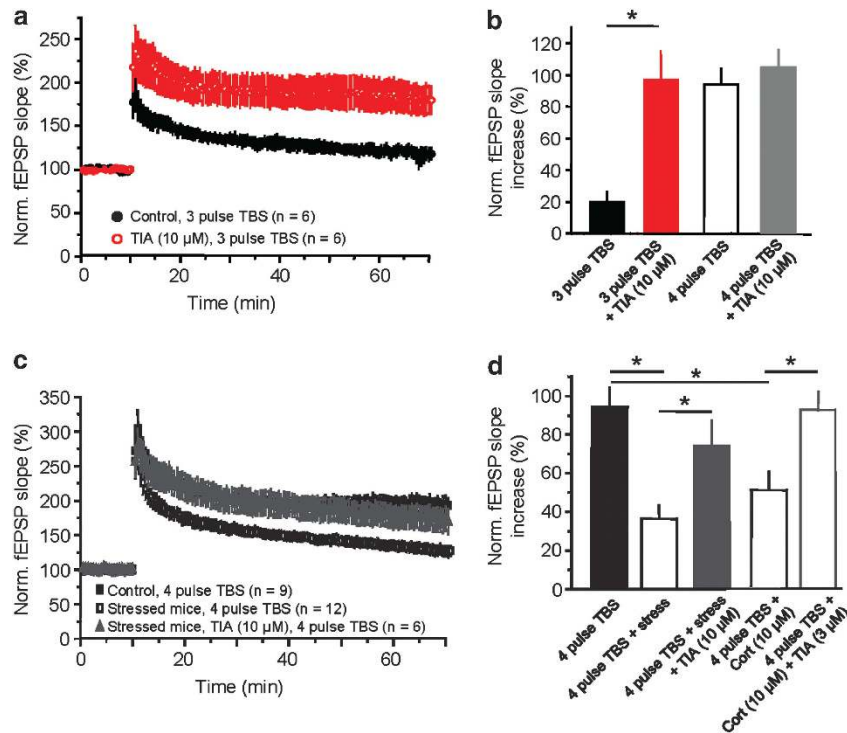
Figure 7. Tianeptine enhances hippocampal CA1 long-term potentiation (LTP) and rescues the suppression of LTP induced by acute stress, or by corticosterone. (**a**) The slope of the field excitatory postsynaptic potentials (fEPSP) (% of the control fEPSP) is plotted as a function of time before and after delivery of a 3-pulse theta burst stimulation (TBS; at $t = 10$ min). The stimulus is designed to induce a submaximal form of LTP (black). Tianeptine (10 μM) greatly enhanced this submaximal LTP (red). Each time point (one every 30 s) represents the mean ± s.e.m. of 6–12 independent experiments. (**b**) The histogram compares the magnitude of LTP (% increase from control of the slope of the fEPSP) determined at 50 min post-TBS and illustrates that a 3-pulse TBS protocol (black) is far less effective in producing LTP than a 4-pulse TBS (white). However, tianeptine (10 μM) greatly increased the magnitude of LTP induced by a 3-pulse TBS to a level similar to that produced by the 4-pulse TBS protocol (red). In contrast to the effect of tianeptine (10 μM) on 3-pulse TBS, this concentration of the drug has no effect on maximal LTP induced by the 4-pulse TBS protocol (gray). Each bar represents the mean ± s.e.m. of six independent experiments (*$P < 0.05$). (**c**) The slope of the fEPSP (% of the control fEPSP) is plotted as a function of time after delivery of a 4-pulse TBS (at $t = 10$ min) for control (black squares), 'stressed' (open squares) and stressed plus 10 μM tianeptine (gray triangles). Note that pre-exposure to acute stress greatly decreased the magnitude of LTP, when compared to that achieved with control neurons. Tianeptine (10 μM) reversed this stress-induced deficit of LTP. Each time point (one every 30 s) represents the mean ± s.e.m. of 6–12 independent experiments. (**d**) The histogram compares the magnitude of LTP determined at 50 min post 4-pulse TBS. Acute stress and corticosterone (10 μM) result in a clear reduction in the extent of LTP when compared to control, which are fully rescued by (10 and 3 μM) tianeptine. Each bar represents the mean ± s.e.m. of 6–12 independent experiments (*$P < 0.05$).

the synapse, that is, the dynamic retention of surface AMPAR in the synapse. Thus, our study provides thus the first evidence that the plastic range of glutamatergic synapses can be preserved by reducing the surface diffusion of AMPAR. It should be noted that tianeptine was more efficient in reducing the diffusion of GluA-AMPAR in synapses than in the extrasynaptic area, consistent with the higher content of PSD-95 in synapses.[65] However, it cannot be excluded that PSD-95 or other scaffold proteins, which have been detected in extrasynaptic areas, provide an additional efficient PDZ domain-containing interactor in the extrasynaptic compartment.[20]

Although the detailed mechanism by which tianeptine favors synaptic plasticity is not fully understood, this and former studies strengthen the view that glutamatergic signaling is the primary target.[29,30] Tianeptine differs from other antidepressants in its pharmacological and neurochemical properties[31] as the drug shows no affinity for known neurotransmitter receptors and does not inhibit the uptake of serotonin or noradrenaline in the central nervous system.[30] Tianeptine increases the phosphorylation of the CaMKII-PKC site (Ser831) of GluA1 subunit in the hippocampus and frontal cortex of mice.[36,50] Consistent with the fact that AMPAR phosphorylation status influence the receptor function,[66,67] tianeptine could increase the AMPAR-mediated EPSC at

the CA3 commissural associational[37] and CA3-CA1 synapses by altering the receptor phosphorylation state. Our data indicate that tianeptine regulates the trafficking and synaptic content of AMPAR through a CaMKII- and stargazin-dependent mechanism that requires the phosphorylation of stargazin and the interaction of the AMPAR/stargazin complex with PDZ scaffold proteins such as PSD-95. It is likely that both processes, that is, change in the single-channel conductance and/or receptor anchoring (this study), occur in parallel and contribute to the increased AMPAR signaling in the presence of tianeptine. Understanding the specific role of each molecular event in tianeptine's effects is of great importance for future therapeutic strategies, but this opportunity remains to be explored. Molecules that appear to favor enhancing AMPAR-mediated current, for example, AMPAkines, have been proven to have antidepressant effects in animal models[68,69] and regulate AMPAR surface diffusion (data not shown), indicating that the glutamate receptor membrane trafficking and the regulatory mechanisms may provide new therapeutic benefits.

Depression is a complex disorder and the cellular mechanisms underlying its pathogenesis have been under considerable scrutiny during the past decades. Chronic stress exposure can favor the appearance of depressive episodes in humans.[70–72] Consequently,
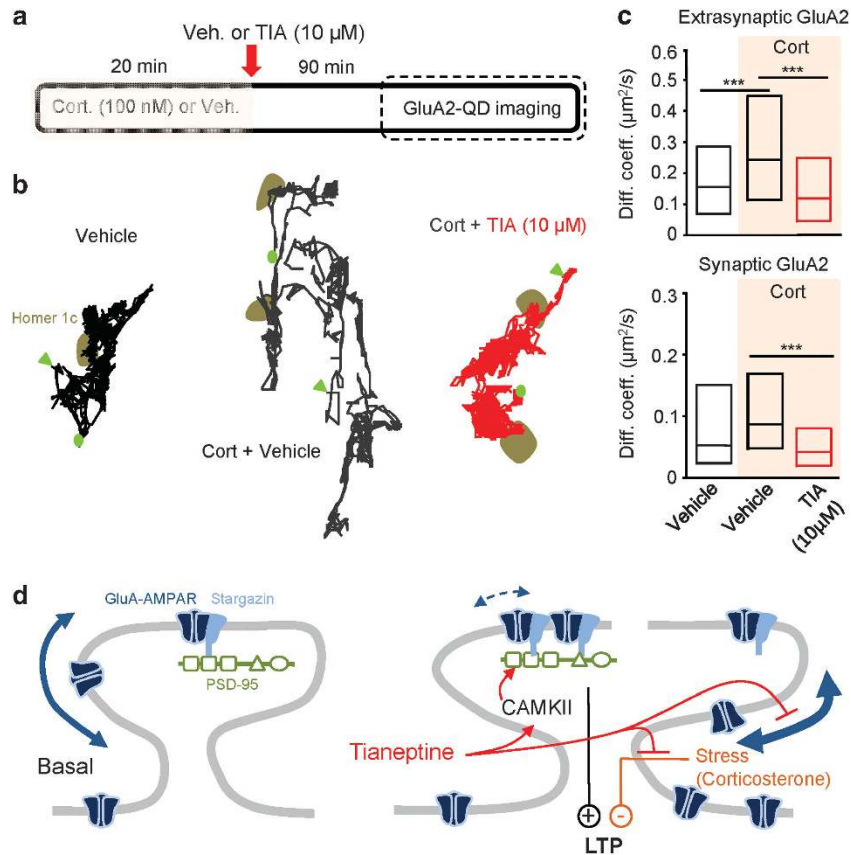
Figure 8. Tianeptine (TIA) prevents corticosterone-induced GluA2- AMPA receptor (AMPAR) surface diffusion increase. Surface GluA2-AMPARs were tracked in the extrasynaptic and synaptic compartments of days in vitro (DIV) 11–12 cultured hippocampal neurons after vehicle/vehicle, corticosterone (Cort)/vehicle or Cort/TIA application. (a) Experimental scheme showing that neurons were incubated with Cort/vehicle (phosphate-buffered saline (PBS)) for 20 min, washed, incubated with TIA (10 μM)/vehicle (H_2O) for 90 min, washed and then tracked for 15–30 min. (b) Representative trajectories (20–40 s) of single surface GluA2-AMPAR in vehicle/vehicle, Cort/vehicle and Cort/TIA conditions. The first point of the trajectory is represented by an arrowhead and the last point by a filled circle. (c) The diffusion coefficients (median ± 25–75% interquartile range (IQR)) of extrasynaptic and synaptic GluA2-AMPAR were increased in neurons incubated with Cort compared to vehicle-treated neurons. These increases were fully prevented by 10 μM TIA (extrasynaptic: vehicle + vehicle = $0.16 ± 0.08$–$0.29 \mu m^2 s^{-1}$, n = 153; Cort + vehicle = $0.24 ± 0.11$–$0.44 \mu m^2 s^{-1}$, n = 350; Cort + TIA (10 μM) = $0.11 ± 0.05$–$0.26 \mu m^2 s^{-1}$, n = 214; P < 0.001; synaptic: vehicle + vehicle = $0.05 ± 0.025$–$0.16 \mu m^2 s^{-1}$, n = 101; Cort + vehicle = $0.09 ± 0.05$–$0.17 \mu m^2 s^{-1}$, n = 210; Cort + TIA (10 μM) = $0.04 ± 0.02$–$0.08 \mu m^2 s^{-1}$, n = 165; ***P < 0.001). (d) Schematic representation of TIA's effects on AMPAR surface diffusion and synaptic long-term potentiation (LTP).

certain stress paradigms have served as the basis of several animal models of depression in which some long-term alterations of cellular and molecular mechanisms were identified. Although this study only investigated the effect of an antidepressant in an acute situation and on the acute effects of corticosterone, it clearly revealed that tianeptine rapidly modulates the surface glutamatergic signaling through intracellular changes in the phosphorylation of receptor anchoring machinery, further strengthening the observation that the dynamics of AMPAR surface is a primary target of stress hormones.[16] Furthermore, there is increasing evidence that the ability to modify synaptic plasticity is a crucial feature of clinically effective antidepressants.[30] Because glutamatergic signaling is a key system in many forms of adaptive cellular plasticity and cognitive functions, it certainly represents a viable downstream target for antidepressant drugs. Conceptually, it emerges that antidepressants can either target first the mono-amine systems, which will subsequently modulate glutamatergic signaling, or directly target glutamatergic signaling. In this respect, tianeptine and the research associated with this compound have pioneered this view since the monoaminergic hypothesis of depression, for example, a serotonergic deficit, cannot explain the antidepressant activity of this drug. Its ability to restore normal neuroplasticity in limbic brain regions[15,36] and plasticity at glutamatergic synapses opens numerous novel therapeutic perspectives to target specifically regulatory elements of glutamatergic signaling. This study clearly emphasizes the positive role of a drug that impacts on AMPAR trafficking. Counteracting the effect of corticosterone on glutamate receptor trafficking in synapses such as after stress events, tianeptine preserves the plastic range of excitatory connections and probably constitutes a cellular substrate to improve the cognitive functions that are altered in stress and depression.

CONFLICT OF INTEREST

The authors declare no conflict of interest.

REFERENCES

1 Agid Y, Buzsaki G, Diamond DM, Frackowiak R, Giedd J, Girault JA et al. How can drug discovery for psychiatric disorders be improved? Nat Rev Drug Discov 2007; 6: 189–201.

2 Krishnan V, Nestler EJ. The molecular neurobiology of depression. Nature 2008; 455: 894–902.

3 Yuksel C, Ongur D. Magnetic resonance spectroscopy studies of glutamate-related abnormalities in mood disorders. Biol Psychiatry 2010; 68: 785–794.

4 Du J, Suzuki K, Wei Y, Wang Y, Blumenthal R, Chen Z et al. The anticonvulsants lamotrigine, riluzole, and valproate differentially regulate AMPA receptor membrane localization: relationship to clinical effects in mood disorders. Neuropsychopharmacology 2007; 32: 793–802.

5 Svenningsson P, Tzavara ET, Witkin JM, Fienberg AA, Nomikos GG, Greengard P. Involvement of striatal and extrastriatal DARPP-32 in biochemical and behavioral effects of fluoxetine (Prozac). Proc Natl Acad Sci USA 2002; 99: 3182–3187.

6 Skolnick P, Popik P, Trullas R. Glutamate-based antidepressants: 20 years on. Trends Pharmacol Sci 2009; 30: 563–569.

7 Berton O, Nestler EJ. New approaches to antidepressant drug discovery: beyond monoamines. Nat Rev Neurosci 2006; 7: 137–151.

8 Manji HK, Drevets WC, Charney DS. The cellular neurobiology of depression. Nat Med 2001; 7: 541–547.

9 Spedding M, Jay T, Costa e Silva J, Perret L. A pathophysiological paradigm for the therapy of psychiatric disease. Nat Rev Drug Discov 2005; 4: 467–476.

10 Rocher C, Spedding M, Munoz C, Jay TM. Acute stress-induced changes in hippocampal/prefrontal circuits in rats: effects of antidepressants. Cereb Cortex 2004; 14: 224–229.

11 Chaouloff F. Serotonin, stress and corticoids. J Psychopharmacol 2000; 14: 139–151.

12 Sahay A, Hen R. Adult hippocampal neurogenesis in depression. Nat Neurosci 2007; 10: 1110–1115.

13 Leuner B, Gould E. Structural plasticity and hippocampal function. Annu Rev Psychol 2010; 61: 111–140, C1–3.

14 McEwen BS. Physiology and neurobiology of stress and adaptation: central role of the brain. Physiol Rev 2007; 87: 873–904.

15 Jay TM, Rocher C, Hotte M, Naudon L, Gurden H, Spedding M. Plasticity at hippocampal to prefrontal cortex synapses is impaired by loss of dopamine and stress: importance for psychiatric diseases. Neurotox Res 2004; 6: 233–244.

16 Chaouloff F, Groc L. Temporal modulation of hippocampal excitatory transmission by corticosteroids and stress. Front Neuroendocrinol 2011; 32: 25–42.

17 Krugers HJ, Hoogenraad CC, Groc L. Stress hormones and AMPA receptor trafficking in synaptic plasticity and memory. Nat Rev Neurosci 2010; 11: 675–681.

18 Hu H, Real E, Takamiya K, Kang MG, Ledoux J, Huganir RL et al. Emotion enhances learning via norepinephrine regulation of AMPA-receptor trafficking. Cell 2007; 131: 160–173.

19 Groc L, Choquet D. AMPA and NMDA glutamate receptor trafficking: multiple roads for reaching and leaving the synapse. Cell Tissue Res 2006; 326: 423–438.

20 Newpher TM, Ehlers MD. Glutamate receptor dynamics in dendritic microdomains. Neuron 2008; 58: 472–497.

21 Jaskolski F, Henley JM. Synaptic receptor trafficking: the lateral point of view. Neuroscience 2009; 158: 19–24.

22 Elias GM, Nicoll RA. Synaptic trafficking of glutamate receptors by MAGUK scaffolding proteins. Trends Cell Biol 2007; 17: 343–352.

23 Shepherd JD, Huganir RL. The cell biology of synaptic plasticity: AMPA receptor trafficking. Annu Rev Cell Dev Biol 2007; 23: 613–643.

24 Groc L, Choquet D, Chaouloff F. The stress hormone corticosterone conditions AMPAR surface trafficking and synaptic potentiation. Nat Neurosci 2008; 7: 695–696.

25 Martin S, Henley JM, Holman D, Zhou M, Wiegert O, van Spronsen M et al. Corticosterone alters AMPAR mobility and facilitates bidirectional synaptic plasticity. PLoS ONE 2009; 4: e4714.

26 Meneses A. Tianeptine: 5-HT uptake sites and 5-HT(1-7) receptors modulate memory formation in an autoshaping Pavlovian/instrumental task. Neurosci Biobehav Rev 2002; 26: 309–319.

27 Jaffard R, Mocaer E, Poignant JC, Micheau J, Marighetto A, Meunier M et al. Effects of tianeptine on spontaneous alternation, simple and concurrent spatial discrimination learning and on alcohol-induced alternation deficits in mice. Behav Pharmacol 1991; 2: 37–46.

28 Zoladz PR, Park CR, Munoz C, Fleshner M, Diamond DM. Tianeptine: an antidepressant with memory-protective properties. Curr Neuropharmacol 2008; 6: 311–321.

29 Diamond DM, Campbell A, Park CR, Vouimba RM. Preclinical research on stress, memory, and the brain in the development of pharmacotherapy for depression. Eur Neuropsychopharmacol 2004; 14(Suppl 5): S491–S495.

30 McEwen BS, Chattarji S, Diamond DM, Jay TM, Reagan LP, Svenningsson P et al. The neurobiological properties of tianeptine (Stablon): from monoamine hypothesis to glutamatergic modulation. Mol Psychiatry 2010; 15: 237–249.

31 Kato G, Weitsch AF. Neurochemical profile of tianeptine, a new antidepressant drug. Clin Neuropharmacol 1988; 11(Suppl 2): S43–S50.

32 McEwen BS, Olie JP. Neurobiology of mood, anxiety, and emotions as revealed by studies of a unique antidepressant: tianeptine. Mol Psychiatry 2005; 10: 525–537.

33 Shakesby AC, Anwyl R, Rowan MJ. Overcoming the effects of stress on synaptic plasticity in the intact hippocampus: rapid actions of serotonergic and antidepressant agents. J Neurosci 2002; 22: 3638–3644.

34 Vouimba RM, Munoz C, Diamond DM. Differential effects of predator stress and the antidepressant tianeptine on physiological plasticity in the hippocampus and basolateral amygdala. Stress 2006; 9: 29–40.

35 Campbell AM, Park CR, Zoladz PR, Munoz C, Fleshner M, Diamond DM. Pre-training administration of tianeptine, but not propranolol, protects hippocampus-dependent memory from being impaired by predator stress. Eur Neuropsychopharmacol 2008; 18: 87–98.

36 Svenningsson P, Bateup H, Qi H, Takamiya K, Huganir RL, Spedding M et al. Involvement of AMPA receptor phosphorylation in antidepressant actions with special reference to tianeptine. Eur J Neurosci 2007; 26: 3509–3517.

37 Kole MH, Swan L, Fuchs E. The antidepressant tianeptine persistently modulates glutamate receptor currents of the hippocampal CA3 commissural associational synapse in chronically stressed rats. Eur J Neurosci 2002; 16: 807–816.

38 Szegedi V, Juhasz G, Zhang X, Barkoczi B, Qi H, Madeira A et al. Tianeptine potentiates AMPA receptors by activating CaMKII and PKA via the p38, p42/44 MAPK and JNK pathways. Neurochem Int 2011; 59: 1109–1122.

39 Banker GA, Cowan WM. Rat hippocampal neurons in dispersed cell culture. Brain Res 1977; 126: 397–342.

40 Groc L, Heine M, Cognet L, Brickley K, Stephenson FA, Lounis B et al. Differential activity-dependent regulation of the lateral mobilities of AMPA and NMDA receptors. Nat Neurosci 2004; 7: 695–696.

41 Tardin C, Cognet L, Bats C, Lounis B, Choquet D. Direct imaging of lateral movements of AMPA receptors inside synapses. EMBO J 2003; 22: 4656–4665.

42 Hollman M, Heinemann S. Cloned glutamate receptors. Ann Rev Neurosci 1994; 17: 31–108.

43 Bats C, Groc L, Choquet D. The interaction between Stargazin and PSD-95 regulates AMPA receptor surface trafficking. Neuron 2007; 53: 719–734.

44 Ehlers MD, Heine M, Groc L, Lee MC, Choquet D. Diffusional trapping of GluR1 AMPA receptors by input-specific synaptic activity. Neuron 2007; 54: 447–460.

45 Makino H, Malinow R. AMPA receptor incorporation into synapses during LTP: the role of lateral movement and exocytosis. Neuron 2009; 64: 381–390.

46 Opazo P, Labrecque S, Tigaret CM, Frouin A, Wiseman PW, De Koninck P et al. CaMKII triggers the diffusional trapping of surface AMPARs through phosphorylation of stargazin. Neuron 2010; 67: 239–252.

47 Heine M, Groc L, Frischknecht R, Beique JC, Lounis B, Rumbaugh G et al. Surface mobility of postsynaptic AMPARs tunes synaptic transmission. Science 2008; 320: 201–205.

48 Groc L, Lafourcade M, Heine M, Renner M, Racine V, Sibarita JB et al. Surface trafficking of neurotransmitter receptor: comparison between single-molecule/quantum-dot strategies. J Neurosci 2007; 27: 12433–12437.

49 Ashby MC, Ibaraki K, Henley JM. It's green outside: tracking cell surface proteins with pH-sensitive GFP. Trends Neurosci 2004; 27: 257–261.

50 Qi H, Mailliet F, Spedding M, Rocher C, Zhang X, Delagrange P et al. Antidepressants reverse the attenuation of the neurotrophic MEK/MAPK cascade in frontal cortex by elevated platform stress; reversal of effects on LTP is associated with GluA1 phosphorylation. Neuropharmacology 2009; 56: 37–46.

51 Lisman J, Schulman H, Cline H. The molecular basis of CaMKII function in synaptic and behavioural memory. Nat Rev Neurosci 2002; 3: 175–190.

52 Suenaga T, Morinobu S, Kawano K, Sawada T, Yamawaki S. Influence of immobilization stress on the levels of CaMKII and phospho-CaMKII in the rat hippocampus. Int J Neuropsychopharmacol 2004; 7: 299–309.

53 Kessels HW, Kopec CD, Klein ME, Malinow R. Roles of stargazin and phosphorylation in the control of AMPA receptor subcellular distribution. Nat Neurosci 2009; 12: 888–896.

54 Tomita S, Stein V, Stocker TJ, Nicoll RA, Bredt DS. Bidirectional synaptic plasticity regulated by phosphorylation of stargazin-like TARPs. Neuron 2005; 45: 269–277.

55 Griffin BA, Adams SR, Tsien RY. Specific covalent labeling of recombinant protein molecules inside live cells. Science 1998; 281: 269–272.

56 Reznikov LR, Grillo CA, Piroli GG, Pasumarthi RK, Reagan LP, Fadel J. Acute stress-mediated increases in extracellular glutamate levels in the rat amygdala: differential effects of antidepressant treatment. Eur J Neurosci 2007; 25: 3109–3114.

57 Reagan LP, Rosell DR, Wood GE, Spedding M, Munoz C, Rothstein J et al. Chronic restraint stress up-regulates GLT-1 mRNA and protein expression in the rat hippocampus: reversal by tianeptine. Proc Natl Acad Sci USA 2004; 101: 2179–2184.

58 Greger IH, Esteban JA. AMPA receptor biogenesis and trafficking. *Curr Opin Neurobiol* 2007; **17**: 289–297.

59 Neves G, Cooke SF, Bliss TV. Synaptic plasticity, memory and the hippocampus: a neural network approach to causality. *Nat Rev Neurosci* 2008; **9**: 65–75.

60 Malinow R, Malenka RC. AMPA receptor trafficking and synaptic plasticity. *Annu Rev Neurosci* 2002; **25**: 103–126.

61 Ashby MC, Maier SR, Nishimune A, Henley JM. Lateral diffusion drives constitutive exchange of AMPA receptors at dendritic spines and is regulated by spine morphology. *J Neurosci* 2006; **26**: 7046–7055.

62 Choquet D. Fast AMPAR trafficking for a high-frequency synaptic transmission. *Eur J Neurosci* 2010; **32**: 250–260.

63 Alfarez DN, Wiegert O, Krugers HJ. Stress, corticosteroid hormones and hippocampal synaptic function. *CNS Neurol Disord Drug Targets* 2006; **5**: 521–529.

64 Karst H, Joels M. Corticosterone slowly enhances miniature excitatory postsynaptic current amplitude in mice CA1 hippocampal cells. *J Neurophysiol* 2005; **94**: 3479–3486.

65 Feng W, Zhang M. Organization and dynamics of PDZ-domain-related supramodules in the postsynaptic density. *Nat Rev Neurosci* 2009; **10**: 87–99.

66 Soderling TR, Derkach VA. Postsynaptic protein phosphorylation and LTP. *Trends Neurosci* 2000; **23**: 75–80.

67 Barria A, Derkach V, Soderling T. Identification of the Ca^{2+}/calmodulin-dependent protein kinase II regulatory phosphorylation site in the alpha-amino-3-hydroxyl-5-methyl-4-isoxazole-propionate-type glutamate receptor. *J Biol Chem* 1997; **272**: 32727–32730.

68 Li X, Tizzano JP, Griffey K, Clay M, Lindstrom T, Skolnick P. Antidepressant-like actions of an AMPA receptor potentiator (LY392098). *Neuropharmacology* 2001; **40**: 1028–1033.

69 Farley S, Apazoglou K, Witkin JM, Giros B, Tzavara ET. Antidepressant-like effects of an AMPA receptor potentiator under a chronic mild stress paradigm. *Int J Neuropsychopharmacol* 2010; **13**: 1207–1218.

70 Kendler KS, Karkowski LM, Prescott CA. Causal relationship between stressful life events and the onset of major depression. *Am J Psychiatry* 1999; **156**: 837–841.

71 Caspi A, Sugden K, Moffitt TE, Taylor A, Craig IW, Harrington H et al. Influence of life stress on depression: moderation by a polymorphism in the 5-HTT gene. *Science* 2003; **301**: 386–389.

72 Binder EB, Nemeroff CB. The CRF system, stress, depression and anxiety-insights from human genetic studies. *Mol Psychiatry* 2010; **15**: 574–588.

Supplementary Information accompanies the paper on the Molecular Psychiatry website (http://www.nature.com/mp)